Energetics of the Kuroshio south of Japan

by David Szabo[1] and Georges L. Weatherly[1]

ABSTRACT

Historical GEK data are used to estimate the flow of energy from the mean current to the fluctuations for the surface of the Kuroshio in a region south of Japan. The horizontal transfer components of kinetic energy and temperature variance are calculated and are found to be similar to estimates for the Florida Current. Locally, the components $\overline{u'v'}\ \partial U/\partial y$ and $\overline{u'u'}\ \partial U/\partial x$ dominate the kinetic energy transfer, and usually are of opposite sign. Similar cancellation of the temperature variance transfer terms is indicated, although the seasonal temperature signal may dominate the result. Cross stream and downstream averaging of the total kinetic energy transfer shows regions of significant transfer both to and from the mean flow. The sign of the net kinetic energy transfer over the region studied cannot be determined. However, the importance of the kinetic energy transfer is established by comparison with estimates of the total derivative of mean and fluctuation kinetic energy.

1. Introduction

The interaction of the fluctuating and mean fields of oceanic currents is an important link in understanding the entire ocean circulation. Theoretical studies have shown several mechanisms capable of generating meandering currents, e.g., baroclinic instability (Orlanski, 1969), bottom steering (Niiler and Robinson, 1967; Robinson and Niiler, 1967; Robinson and Taft, 1972), and Rossby lee waves (White and McCreary, 1976). Observational studies, paralleling the theoretical work, have attempted to determine the basic energetic relationship between the mean flow and the fluctuations. The results of such studies have been severely limited, because of the data necessary for significant computations, to parts of only one western boundary current, the Florida Current, and to analysis of only a few of the terms in the energy equations.

The intent of the present study is to make similar estimates for the surface layer of a region of the Kuroshio for comparison with results for the Florida Current. The data we have used allow a more complete analysis of the terms in the energy equations than has been possible for the Florida Current.

The data analysis in past studies and here focuses on estimating several terms

1. Department of Oceanography, Florida State University, Tallahassee, Florida, 32306, U.S.A.

appearing in the equations governing the fluctuating kinetic energy (neglecting the dissipation term) and fluctuating density variance, which are

$$\frac{\partial}{\partial t}\left(\frac{\overline{u_i'u_i'}}{2}\right) + \frac{\partial}{\partial x_j}\left[\overline{u_j'}\,\frac{\overline{u_i'u_i'}}{2} + U_j\frac{\overline{u_i'u_i'}}{2} + \frac{\overline{u_j'p'}}{\rho_0}\right] = -\frac{\overline{u_j'\rho'}}{\rho_0}\,g_j - \overline{u_i'u_j'}\,\frac{\partial U_i}{\partial x_j} \tag{1}$$

$$\frac{\partial}{\partial t}\left(\frac{\overline{\rho'\rho'}}{2}\right) + \frac{\partial}{\partial x_j}\left[U_j\,\frac{\overline{\rho'\rho'}}{2} + \overline{u_j'}\,\frac{\overline{\rho'\rho'}}{2}\right] = -\overline{u_j'\rho'}\,\frac{\partial \rho}{\partial x_j} \tag{2}$$

respectively. Here, $i,j = 1,2,3$; 1,2 = horizontal; 3 = vertical; U_j = the mean velocity components; u'_j = the fluctuating velocity components; p' = the fluctuating pressure; ρ = the mean density; ρ' = the fluctuating density; x_j = the Cartesian coordinates; ρ_0 = the reference density; $g_j = (0,0,g)$ = gravitational acceleration; and an overbar is a time average.

Equations (1) and (2) may be combined (Brooks and Niiler, 1977) into a single conservation equation, for the fluctuating kinetic and potential energies

$$\underbrace{\frac{d}{dt}\left[\frac{\overline{u_i'^2}}{2} - \frac{g}{\rho_0}\,\frac{\overline{\rho'^2}}{2}\Big/\left|\frac{\partial \rho}{\partial z}\right|\right]}_{\text{(a)}} = \underbrace{-\frac{\partial}{\partial x_j}\left(\frac{\overline{u_j'p'}}{\rho_0}\right)}_{\text{(b)}} \underbrace{-\overline{u_i'u_j'}\,\frac{\partial U_i}{\partial x_j}}_{\text{(c)}} \underbrace{-\frac{g}{\rho_0}\,\overline{u_i'\rho'}\,\frac{\partial \rho}{\partial x_i}\Big/\left|\frac{\partial \rho}{\partial z}\right|}_{\text{(d)}} \tag{3}$$

In arriving at this equation, the Boussinesq and hydrostatic approximations have been made, triple products of fluctuating components have been neglected and the term $\frac{\overline{\rho'^2}}{2}\,\frac{g}{\rho_0}\,\frac{d}{dt}\left(1\Big/\left|\frac{\partial \rho}{\partial z}\right|\right)$ has been neglected. Equation (3) states that the change in total fluctuation energy following the mean flow, *a*, is the result of pressure work, *b*, transfer of kinetic energy from the mean flow, *c*, and the transfer of potential energy from the mean flow, *d*.

Table 1 summarizes several terms in the energy equations that have been estimated for the Florida Current. In these studies as in ours, no estimate of the pressure work term (term *b* in Equation 3) has been made. Table 1a lists results for the surface energetics, and Table 1b for calculations which include vertical resolution. The surface energetic calculations by Webster (1961, 1965) and by Schmitz and Niiler (1969) make estimates of one component of the kinetic energy transfer, $\overline{u'v'}\,\partial V/\partial x$, where u' and v' are the fluctuating velocities in the cross and downstream directions respectively and V is the mean downstream velocity. Just this single component could be calculated, but Webster (1961) reasoned that this term should be the most important. The results obtained for the kinetic energy transfer

Table 1. Results for the Florida Current.

1a

Reference	Region of Current	Instrument	Time Span	Averaging Method	Cross Stream Average $\overline{u'v'}\,\partial V/\partial x \times 10^{-4}$ (ergs/cm²s)	$\overline{u'T'}$ (cgs) (surface)	Transfer of available potential energy*
Webster (1965)	Cape Hatteras	GEK	Oct 1962 (3 weeks)	Zonal	82 ± 98		
Oort (1964)	Cape Hatteras	GEK	Oct 1962 (3 weeks)	Zonal	—	1.8 ± 1.3	6×10^{-4}
Webster (1961)	Onslow Bay	GEK	May-June 1958 (4 weeks)	Time	79 ± 30		
Oort (1964)	Onslow Bay	GEK	May-June 1958 (4 weeks)	Time	—	3.5 ± 1.6	3×10^{-4}
Webster (1965)	Jacksonville	GEK	Oct-Nov 1961 (7 weeks)	Time	59 ± 84		
Webster (1965)	Jacksonville	D-R	Oct-Nov 1961 (7 weeks)	Time	48 ± 81		
Oort (1964)	Jacksonville	GEK	Oct-Nov 1961 (7 weeks)	Time	—	.46 ± .55	2×10^{-4}
Schmitz & Niiler (1969)	Jacksonville	Dropsonde	July-Aug 1967	Time	−1 ± 18		
Webster (1961)	Miami	GEK	1952-1958	Zonal	−.2 ± 27		
Schmitz & Niiler (1969)	Miami	Dropsonde	Aug 1964-May 1967	Zonal	.4 ± 8		

1b

Vertical-Cross Stream Average (ergs/cm^{3}s $\times$ 10^{-4})

Reference	Region of current	Instrument	Time Span	$\bar{\rho}\,\overline{u'v'}\,\partial V/\partial x$	$\overline{g\rho'}\,\frac{\partial\bar{\rho}/\partial x}{\partial\bar{\rho}/\partial z}$	$\bar{\rho}\,\overline{u'u'}\,\partial U/\partial x$	$\overline{gv'\rho'}\,\frac{\partial\bar{\rho}/\partial y}{\partial\bar{\rho}/\partial z}$	$\bar{\rho}\,\overline{v'v'}\,\partial V/\partial y$	Total potential transfer	Total kinetic transfer
Brooks & Niiler (1977)	Miami	Dropsonde	May 16-Aug 13, 1974	−.86 ± 15	−6.2 ± 13	2.4 ± 4	6.1 ± 17	.08 ± 13	−.13 ± 30	1.6 ± 32

* >0 indicates transfer to the mean potential energy.

Figure 1. Results for the Florida Current at Miami (Section 1) and Jacksonville (Section 2), from Schmitz and Niiler (1969). Results from GEK measurements (Webster, 1961, 1965) are plotted with squares and brackets indicate the error tolerances. Results from dropsonde measurements (Schmitz and Niiler, 1969) are plotted as dotted lines with dashed lines indicating error tolerances. (a) and (e) are the east-west speeds (cm/s(, (b) and (f) are the north-south speeds (cm/s), (c) and (g) are the Reynolds stress component $\overline{u'v'}$, (cm^2/s^2), (d) and (h) rate of kinetic energy transfer, $\overline{u'v'}\,\partial V/\partial x$, ($10^{-2}$ ergs cm^3/s).

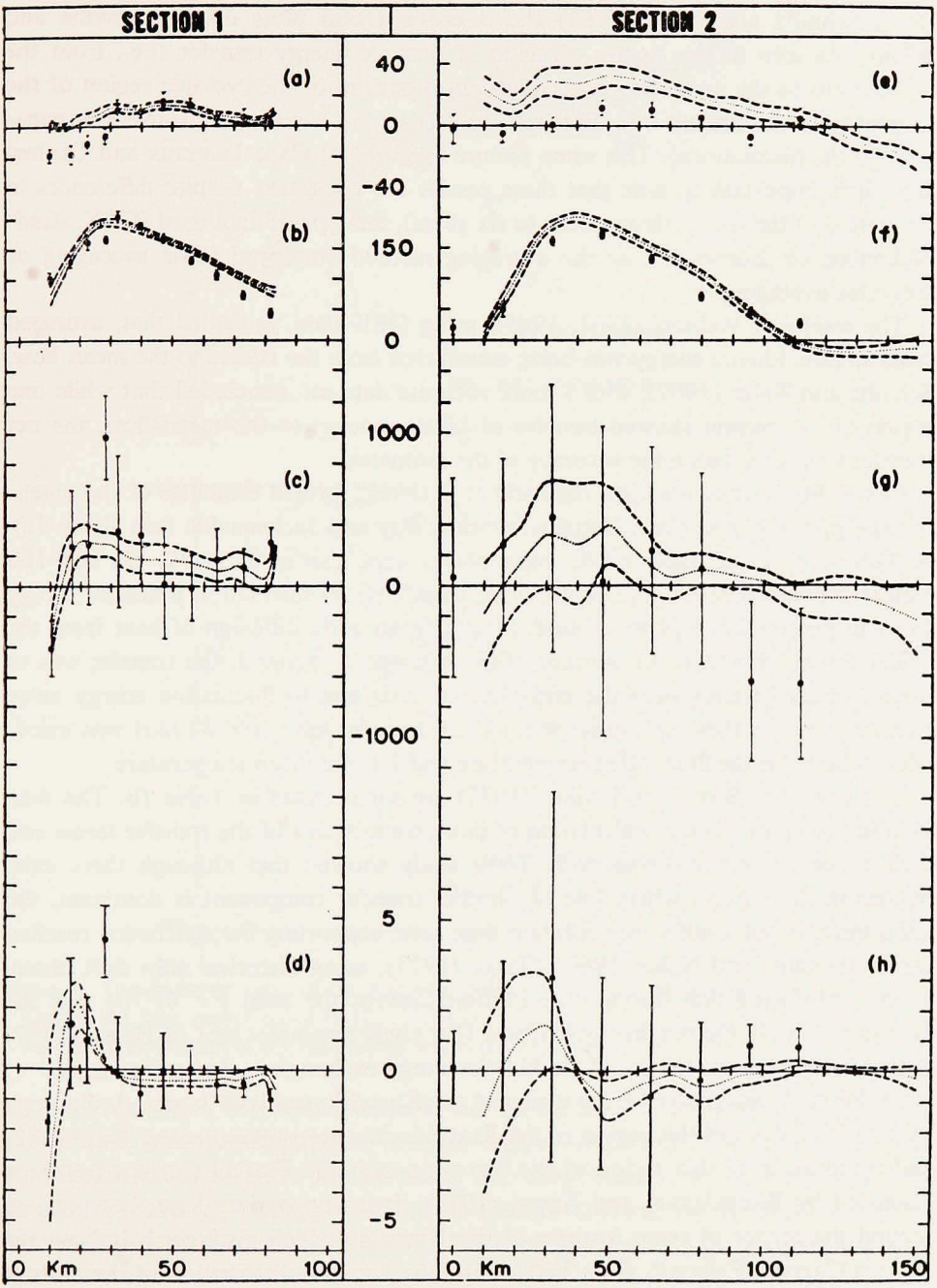
SECTION 1
SECTION 2
(a)
(b)
(c)
(d)
(e)
(f)
(g)
(h)
40
0
-40
150
0
1000
0
-1000
5
0
-5
0 Km 50 100
0 Km 50 100 150

are remarkably similar at each of the four locations in the Florida Current. Figure 1 (from Schmitz and Niiler, 1969) shows cross stream plots off Jacksonville and Miami. As seen in this figure, a region of positive energy transfer (i.e., from the fluctuations to the mean flow) was found in a portion of the cyclonic region of the current near the stream axis. Through the rest of the current, the transfer is negative (to the fluctuations). This same picture emerged at Cape Hatteras and Onslow Bay. It is important to note that these results are consistent despite differences in the period of the mean (three weeks to six years), the type of data used (GEK, dead-reckoning, or dropsonde), or the averaging method employed (time averaging or ensemble averaging).

The results of Webster (1961, 1965), using GEK data, indicated that, averaged cross stream, kinetic energy was being transferred from the eddies to the mean flow. Schmitz and Niiler (1969), with a more accurate data set, concluded that while one region of the current showed transfer of kinetic energy to the mean flow, the net transfer was zero, within the accuracy of the estimates.

Oort (1964), using the same data sets as Webster, formed estimates of the potential energy transfer at Cape Hatteras, Onslow Bay and Jacksonville (see Table 1a). At Onslow Bay and Jacksonville, calculations were also made at 30, 60, and 100 meters. At each location and depth, a net transfer from fluctuation potential energy to mean potential energy was found, indicating an eddy diffusion of heat from the colder inshore water to the warmer offshore water. In general, the transfer was to mean potential energy near the mean current axis and to fluctuation energy away from the axis. In these calculations, only one transfer term ($\overline{u't'}\ \partial T/\partial x$) was calculated, where t' is the fluctuating temperature and T is the mean temperature.

The results of Brooks and Niiler (1977) are summarized in Table 1b. The data used in this study allowed calculation of more components of the transfer terms and their vertical distributions as well. Their study showed that although there exist regions in the current where one or another transfer component is dominant, the net transfer is not significantly different than zero, supporting the conclusion reached earlier (Schmitz and Niiler, 1969). Hager (1977), using historical ship drift observations, estimated that through the Florida Current the term $\overline{v'v'}\ \partial V/\partial y$ was the dominant term in the net energy balance. Our study resembles that of Hager (1977) in that both are areal studies of the kinetic energy exchange in the surface layer.

In this study we report on the region of the Kuroshio south of Japan. A thorough kinematic analysis of this region of the Kuroshio has been presented by Taft (1972) and comparison of this region of the Kuroshio with the Florida Current has been discussed by Worthington and Kawai (1972). It is appropriate here, however, to remind the reader of some features of the Kuroshio which distinguish it from the Florida Current. Figure 2, from Taft, shows the bimodal distribution of the path of the Kuroshio. Similar bimodal behavior is not found in the Florida Current. For reasons discussed later, we have analyzed data only when the Kuroshio was in the

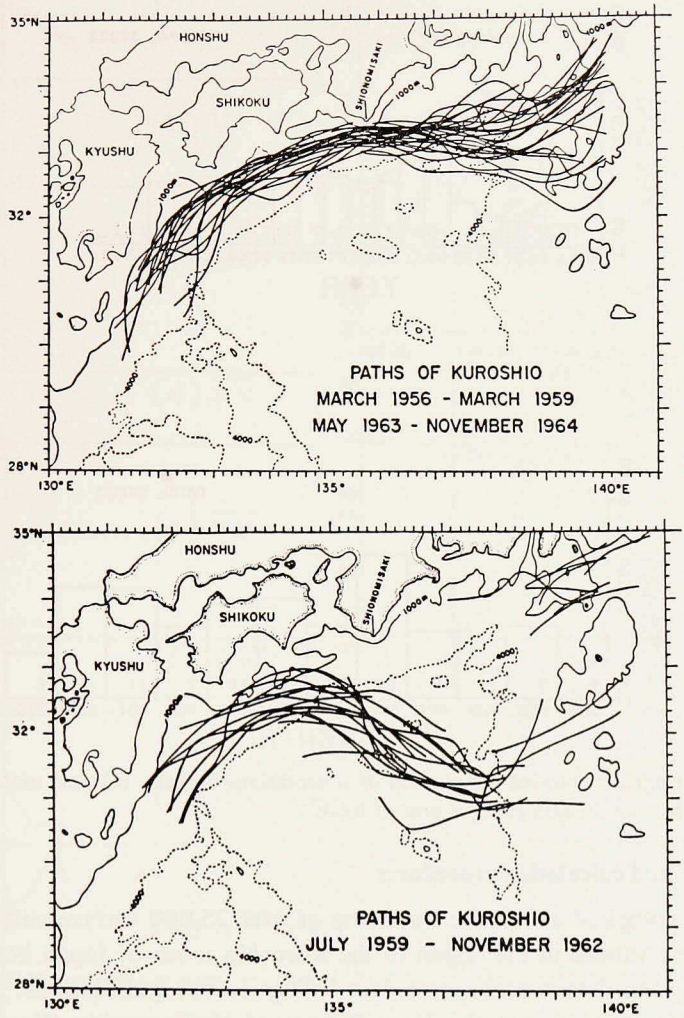

Figure 2. Composite of paths of the Kuroshio during indicated time periods from Taft (1972). During the time period noted in (a), the current was in the 'no meander mode' and during the time period noted in (b), the current was in the 'meander mode.'

'no meander' mode, Figure 2a. When in the 'no meander' mode Cape Shionomisaki at 135°40′E is a separation point, in some ways analogous to Cape Hatteras for the Florida Current, where the current heads into deep water (>4000 m) and its path becomes increasingly variable. Unlike the Florida Current, the Kuroshio re-enters shallow depths (≅1000 m) as it crosses the Izu Ogasawara Ridge at approximately 139°E. As the Kuroshio traverses the region south of Japan the axial speed accelerates from 98 cm/s at 132°15′E to a maximum of 167 cm/s at 137°E and then decelerates to 131 cm/s at 140°E.

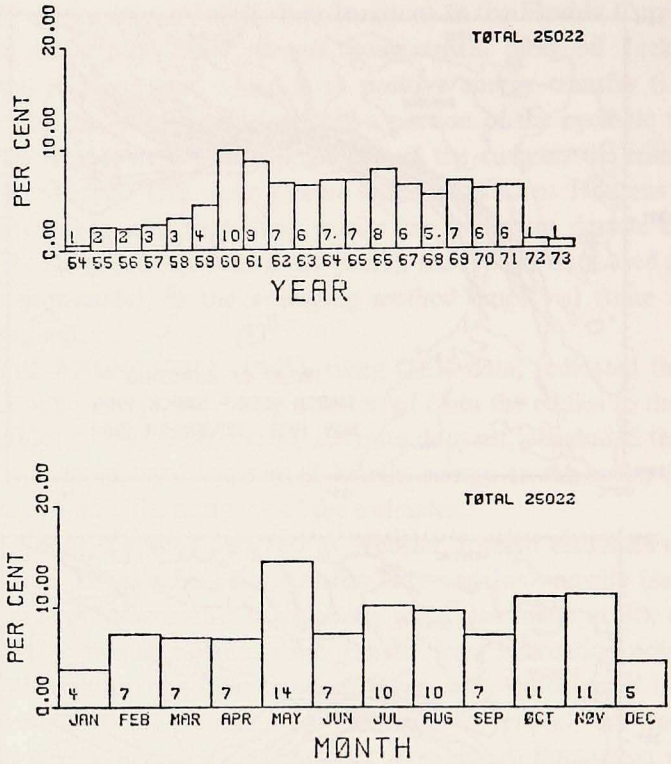

Figure 3. Histograms showing distribution of observations by year, (a), and month, (b), for the data. Numbers inside bars give per cent of total.

2. The data and calculation procedures

We have compiled a data file consisting of over 25,000 surface current and temperature observations in the region of the Kuroshio south of Japan between 130°E and 141°E. The data sources were data listings in two publications: the Japanese Hydrographic Bulletin and the Data Report of Hydrographic Observations. Although the entire set spans the 20-year period 1954 to 1973, 87 per cent is rather evenly spaced through the period 1960 to 1971 (Fig. 3). By month, the data are evenly distributed except that there are slightly fewer observations in the winter months. Several standard sections across the Kuroshio at different longitudes have been occupied on a quarterly basis throughout much of this time period. However, many special cruises have been made so that the data are distributed throughout the region, not just along several transects.

As mentioned in Section 1, data collected during the 'meander' mode were eliminated from the data file before any of the calculations discussed here were made. The data were separated into 'meander' and 'no meander' modes based on Taft (1972) and visual inspection of monthly vector plots of the data for data not included

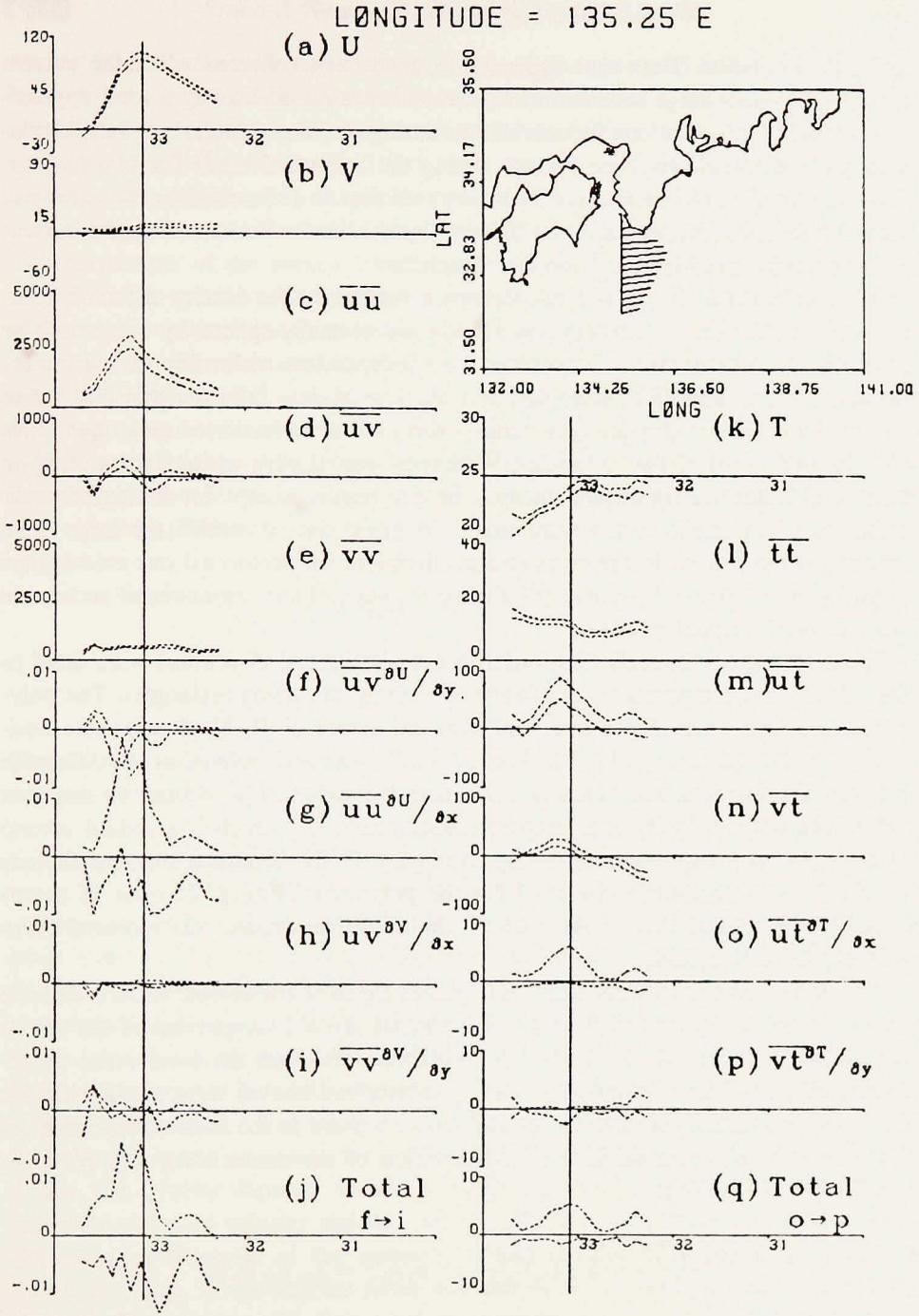

Figure 4. Results at longitude 135.25°E versus latitude (°N). Units are cgs and °C for (a) - (n). Units for (o) - (q) are 10^{-5}(°C)^2/s. The symmetric error bounds are plotted as dashed lines. North-south separation of data points is .1° latitude. Solid line through graphs indicates axis of mean current. The chartlet shows the location of the section and a stick plot of the mean current.

in Taft's discussion. Data that appeared to have been collected while the current was in a transient stage between modes were also removed leaving a total approximately 16,000 observations for calculation during the 'no meander' mode. Calculations were not made for time periods during the 'meander' mode for two reasons. First, the number of observations were not sufficient to form reliable estimates and second, the main current was often 'missed' by the data collectors when the current had apparently meandered beyond their reach.

The spatial resolution of our calculations is limited by the density of the observations. Sequential observations at any section are normally spaced by one month or more and we assume each observation is an independent realization of the instantaneous current. Ensemble averaging over all time of data falling within 0.3 degree latitude by 0.5 degree longitude rectangles was used to estimate the mean quantities at the center point of the rectangles. We experimented with various size averaging areas and found no significant changes in our results except for increased error estimates when smaller areas were used. To more clearly resolve the large scale features of the current in the cross stream direction, we performed our calculations at grid points separated by only 0.1 degrees latitude. Thus, estimates at successive grid points are not independent.

Least-square polynomials (first order in both horizontal directions) were fitted to the velocity and temperature data for each of the overlapping rectangles. The polynomial fits thus define the means and standard errors of U, V, T and their horizontal gradients at each grid point. The fluctuations were calculated as the difference between the instantaneous measurement and the polynomial closest to the data point. The mean velocity and temperature covariances (and their standard errors) at each grid point were calculated by averaging all the instantaneous correlations within the same rectangle size used for the polynomial fitting. Because of downstream ($\cong$ east) variation of the current, the above procedure was repeated every 0.25 degrees of longitude.

The Kuroshio changes direction as it passes through the region studied and the mean current at any transect is not unidirectional. To aid comparison of the results at different locations we have used a coordinate based on the local mean downstream velocity. The original computations (described above) were made with one Cartesian coordinate and then these results were rotated to the local downstream coordinate (e.g., U, x are positive in the direction of the mean flow). The rotations used may be defined as:

$$\frac{\partial U_i^*}{\partial x_j} = \lambda_{iq}\,\lambda_{jk}\frac{\partial U_q}{\partial x_k}; \quad \overline{u_i'u_j'}^* = \lambda_{iq}\,\lambda_{jk}\,\overline{u_q'u_k'}$$

$$\frac{\partial T^*}{\partial x_i} = \lambda_{ij}\frac{\partial T}{\partial x_j}; \quad \overline{u_i't'}^* = \lambda_{ij}\,\overline{u_j't'} \tag{4}$$

where ′ * ′ indicates the rotated tensor; T, t' are the mean and fluctuating temperatures; λ is the two-dimensional rotation tensor; $i,j,q,k, = 1,2$; θ is the angle of rotation; and U_i, u_i are the horizontal mean and fluctuation speeds. After the rotation of gradients and covariances (and their error bounds) were made, the energy transfer terms were calculated by simple multiplication.

It is important to note that the total fluctuating kinetic energy, and the sum of the components of the energy transfer, are independent of the coordinate system used and thus remain unchanged after rotation. However, the magnitude and sign of the components of energy transfer are highly dependent on the coordinate used. Thus, the use of local downstream coordinates makes the interpretation of the transfer terms clearer (e.g., $\overline{u'v'}\ \partial U/\partial y$ is transfer due to local cross stream effects) and facilitates comparison of results at different locations.

The error bounds on the transfer terms have been estimated by assuming the Reynolds stress and the velocity gradient are not independent, i.e., we have calculated the error (ERR) as:

$$ERR\left(\overline{u_iu_j}\,\frac{\partial U_i}{\partial x_j}\right) = ERR\,(\overline{u_iu_j}) \cdot \frac{\partial U_i}{\partial x_j} + \overline{u_iu_j} \cdot ERR\left(\frac{\partial U_i}{\partial x_j}\right) + ERR\,(\overline{u_iu_j}) \cdot ERR\left(\frac{\partial U_i}{\partial x_j}\right) \tag{5}$$

The error on the sum of the transfer terms has been estimated by assuming independence of the terms, i.e.,

$$ERR\left(\sum_{i,j}\ \overline{u_iu_j}\,\frac{\partial U_i}{\partial x_j}\right) = \left[\sum_{i,j}\left[ERR\left(\overline{u_iu_j}\,\frac{\partial U_i}{\partial x_j}\right)\right]^2\right]^{\frac{1}{2}} \tag{6}$$

The instrumental error is excluded in the error estimates. Random measurement error is reduced in the averaging of the mean velocities, temperatures, and auto covariances. However, random errors will tend to increase the auto covariances.

A significant source of error is a depth bias of the GEK. In GEK velocity measurements, the measured velocity is corrected by multiplication with an empirical k-factor. The k-factor is usually determined by comparison of the raw GEK velocity with a measurement using another method, e.g., ship drift. The data used in this investigation have been corrected with a constant k-factor (Taft, 1972, p. 176). In reality, the k-factor depends on several parameters including most importantly the vertically averaged velocity and the surface velocity. The dependence is that k decreases when the ratio of the vertically averaged velocity to the surface velocity decreases. Thus, as the current flows into deeper water without change in surface velocity, the k-factor will then tend to overestimate velocities in deeper water. Teramoto's (1971) estimates for the Kuroshio show that if a current with a ratio of the vertically averaged velocity to surface velocity of 1/3.5 in water 2000 m deep

entered water 4000 m deep with no changes in surface speed, the k-factor would change by about 10 per cent. Thus, errors in measurement of the surface velocities, dependent primarily on location, are probably 10 per cent. This error will have its most significant effect on the velocity derivatives in the direction of changing depth.

The topography beneath the Kuroshio in the region studied is quite complex. Since we have averaged the velocities over an area of 0.3 degrees latitude and 0.5 degrees longitude, we must view the topographic effect on the k-factor similarly averaged. The current follows the continental slope, at a depth of about 1000 m, until it passes Shionomisaki. On the anticyclonic side of the current in this region, the gradient $\partial U/\partial y$ is large and of the order 10^{-5} s^{-1}, i.e., the downstream velocity decreases from about 110 cm/s at the current axis to about 60 cm/s in about 50 km in the cross stream direction. In that distance, the depth roughly doubles from 2000 m to 4000 m. Assuming Teramoto's estimate, the error in $\partial U/\partial y$ is 10^{-6} s^{-1} or 10 per cent. On the cyclonic side of the current, the cross stream gradient of the topography is generally less than on the anticyclonic side while $\partial U/\partial y$ is larger, so we expect the error is less. The downstream gradient $\partial U/\partial x$ is approximately an order of magnitude lower than $\partial U/\partial y$ so the error caused by the constant k-factor is relatively larger if the downstream depth gradient is comparable to the cross stream gradient. The steepest depth gradient in the direction of the flow is between 136°E and 137°E, where the depth changes from 2000 m to 4000 m in a distance of 100 km. This depth change can account for an error in $\partial U/\partial x$ along the axis of about 10^{-6} s^{-1}. Therefore, in this region the sign of $\partial U/\partial x$ may be in error because of the use of a constant k-factor.

3. Results

In this section, the calculated variables are presented and discussed. In Figures 4 and 5 the results, plus and minus the standard error, at two transects are presented. The location of the axis is indicated by a solid line that runs through all graphs (see Szabo, 1978, for more cross stream plots). The results are all rotated to the local mean downstream coordinate except for the U and V velocity components which are in the usual east, north coordinates. In these figures and all subsequent figures, results are presented only if the number of measurements used to form an estimate was equal to or greater than 50. Since the data are concentrated in the region between 134.0°E and 138.0°E, energy calculations are presented only for this region. The average number of observations per calculation point over the region bounded by 134.0°E to 138.0°E is 125.

The mean flow is presented in Figure 6 for all data compiled during the 'no meander' mode. The width of the mean current is given in Table 2; it is arbitrarily taken as the distance between 25 cm/s isotach on the cyclonic side of the Kuroshio and 60 cm/s isotach on the anticyclonic side of the Kuroshio. The 25 cm/s bound

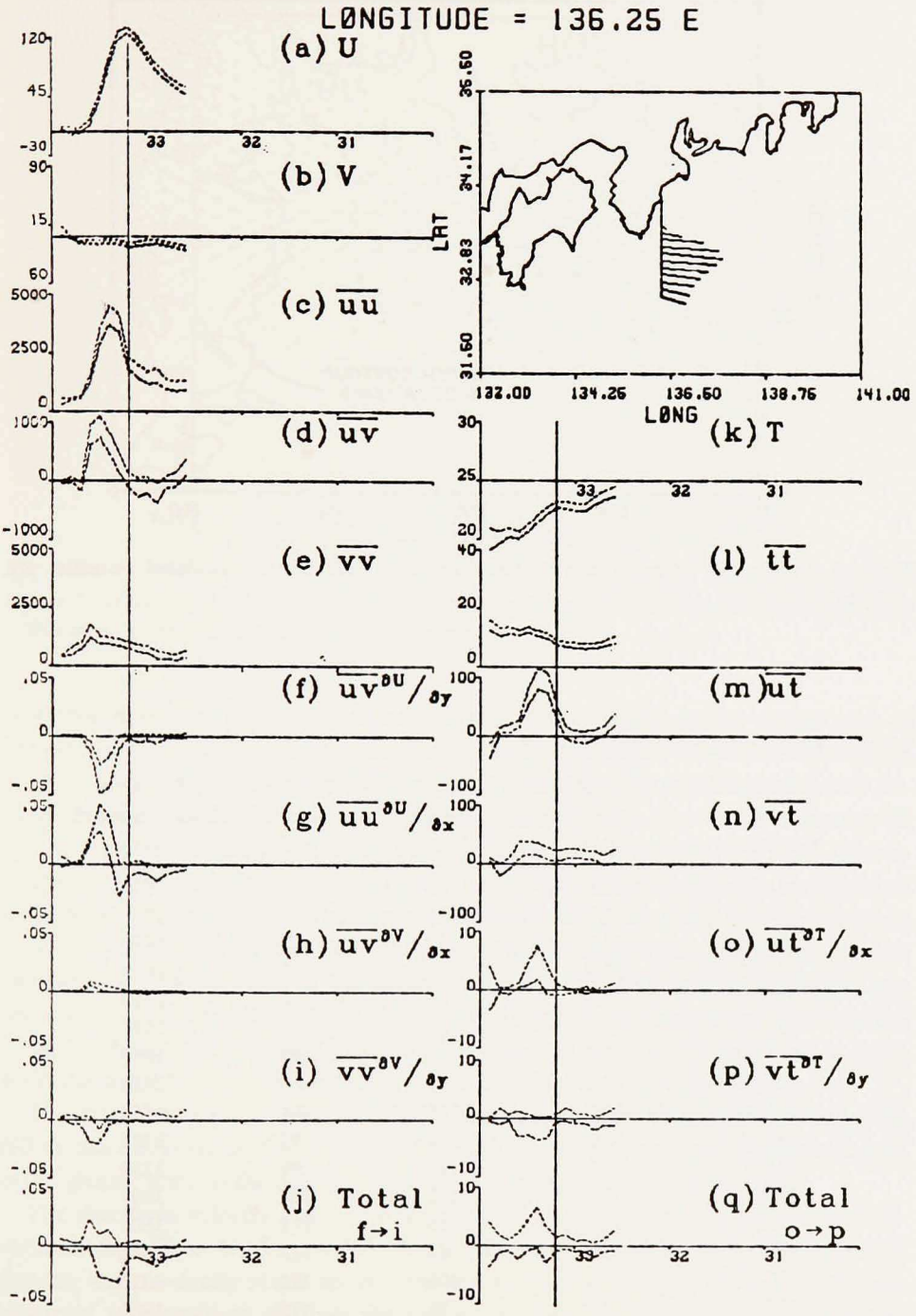

Figure 5. Results at longitude 136.25°E versus latitude (°N). See Fig. 4 for further explanation.

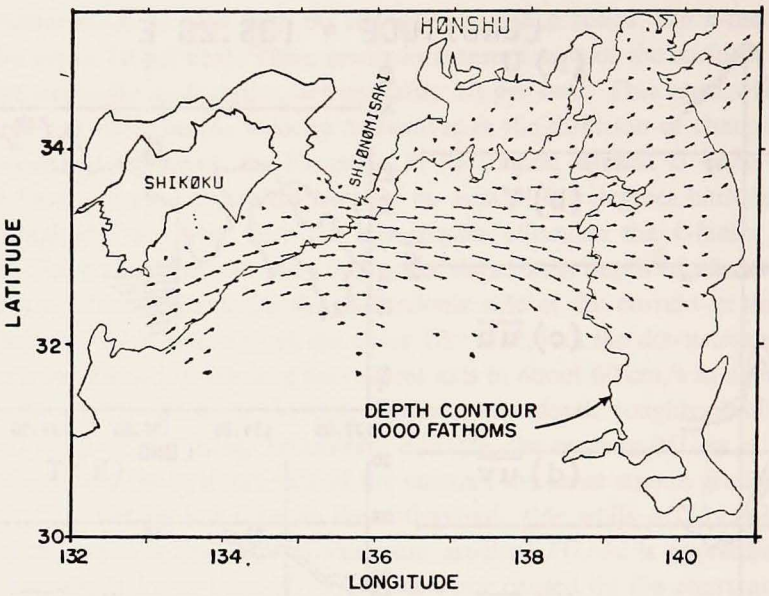

Figure 6. Vector plot of mean current. (For visibility, half of the calculated velocities are plotted.)

Table 2. Characteristics of the mean current.

Longitude	Latitude at axis (°N)	Axial speed (cm/s)	Width of current (km)	Depth to bottom beneath axis (m)
134.00	32.8	95		1100
134.25	32.8	93	93	1250
134.50	32.9	95	87	1450
134.75	32.9	91	92	1650
135.00	33.0	86	94	1750
135.25	33.1	94	97	1550
135.50	33.1	103	93	1650
135.75	33.2	115	83	2150
136.00	33.2	125	101	1650
136.25	33.2	129	97	2050
136.50	33.2	120	99	2750
136.75	33.2	112	104	3000
137.00	33.15	116	112	3500
137.25	33.1	115	119	4000
137.50	33.1	106	122	4000
137.75	33.1	97	125	3600
138.00	33.0	87	132	4000

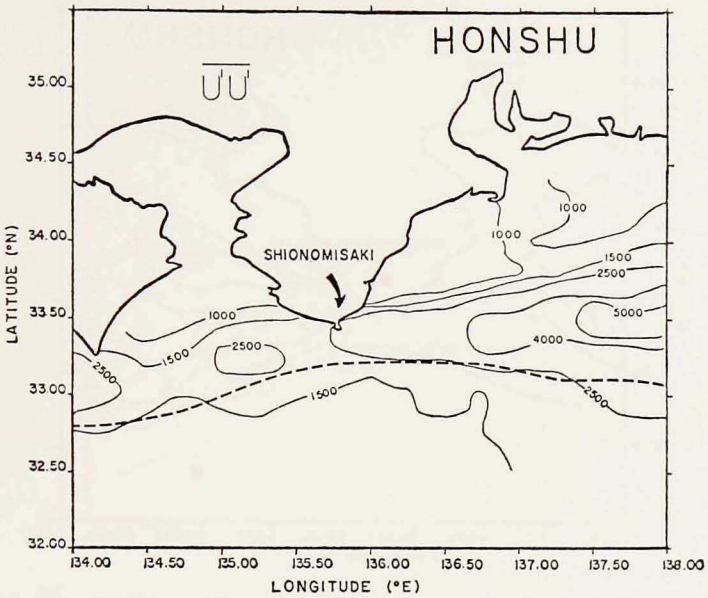

Figure 7. Distribution of the local downstream velocity auto covariance, $\overline{u'u'}$ (cm²/s²). Note that contours are not drawn at regular intervals.

was chosen so that the energy transfer north of the current in the region east of Shionomisaki could be eliminated. The seaward bound of 60 cm/s was chosen because seaward of this isotach, data are not available at many longitudes and because the energy transfer is insignificant past this isotach. The width decreases at 135.75°E (Shionomisaki) as does the instantaneous width (Taft, 1972). Downstream of Shionomisaki the width of the mean current increases due to increased meandering of the current. The mean axial speed increases from west to east to a maximum at 136.25°E and then decreases further to the east. This result is the combination of a reflection of the instantaneous current speed which attains a maximum at 137.0°E and the fact that the current meanders increase in amplitude downstream of Shionomisaki. North of the Kuroshio and east of Shionomisaki a mean southwestward flow, characterized by speeds of 10-15 cm/s is observed.

The mean temperature shows little downstream change. The isotherms generally follow the direction of the current. The cross stream temperature gradient is generally greater than on the cyclonic side of the current (see Figs. 4k and 5k).

The dominant velocity auto covariance is $\overline{u'u'}$, the local downstream velocity covariance (see Figs. 4c, 5c, and 7). A maximum in $\overline{u'u'}$ is found in the region of greatest mean velocity shear on the cyclonic side of the current which changes significantly in magnitude through the region of observation. West of Shionomisaki there are significant oscillations of the maximum. The local cross stream velocity

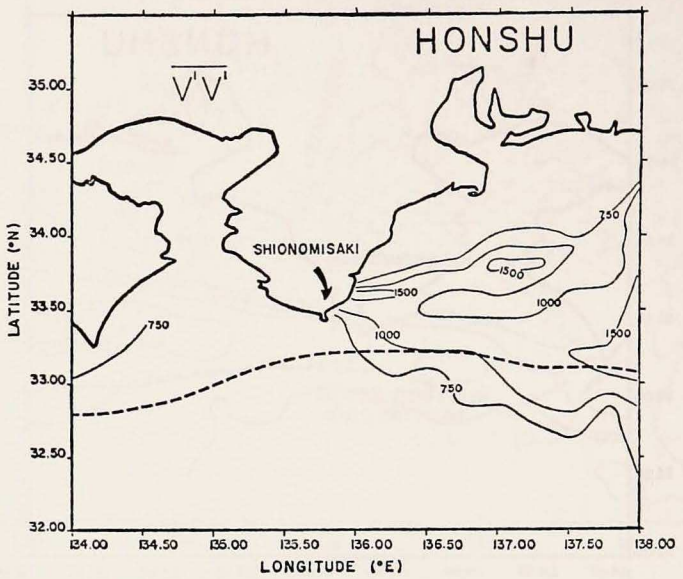

Figure 8. Distribution of the local cross stream velocity auto covariance, $\overline{v'v'}$ (cm^2/s^2). Note that contours are not drawn at regular intervals.

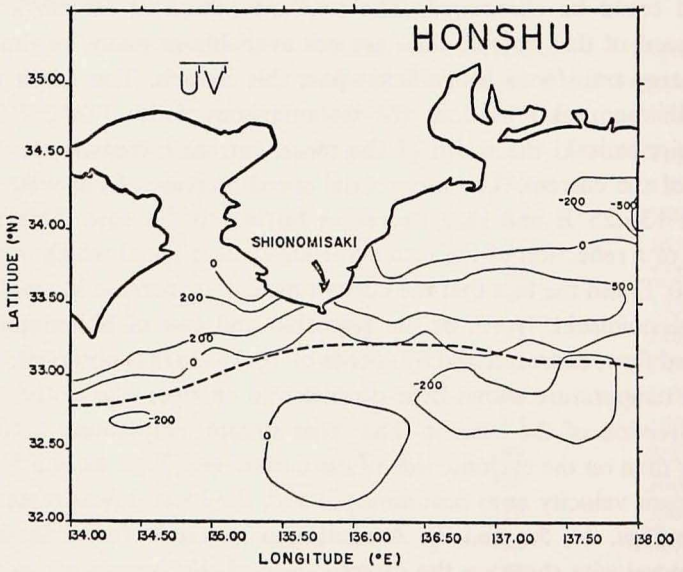

Figure 9. Distribution of the local cross covariance, $\overline{u'v'}$ (cm^2/s^2). Note that contours are not drawn at regular intervals.

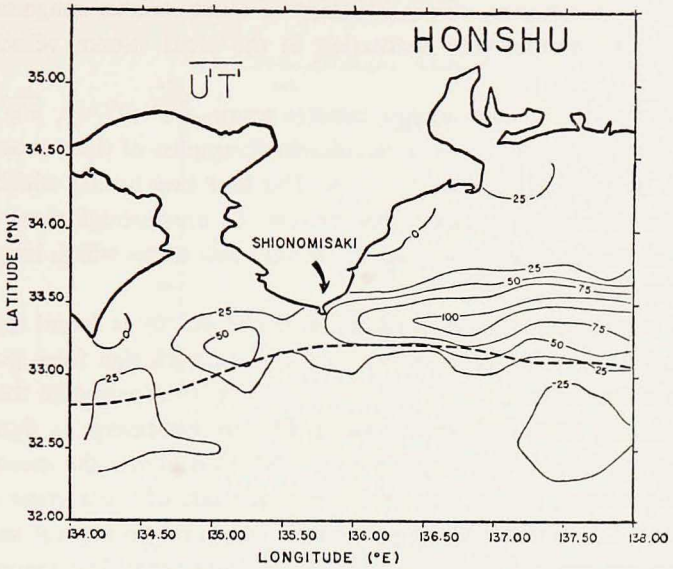

Figure 10. Distribution of the local downstream velocity-temperature covariance, $\overline{u't'}$ (cm°C/s).

covariance (Fig. 8), $\overline{v'v'}$, is generally one-half to one-fifth the magnitude of $\overline{u'u'}$ in in the major portion of the current. West of Shionomisaki there is little change in $\overline{v'v'}$ in either the cross stream or downstream directions. Downstream of Shionomisaki $\overline{v'v'}$ increases on the cyclonic side of the current.

The local velocity cross covariance (Fig. 9), $\overline{u'v'}$, is generally positive on the cyclonic side of the current and negative on the anticyclonic side of the current. Near the northern edge of the current and near the axis, $\overline{u'v'}$ crosses from positive to negative. A positive maximum on the cyclonic portion of the current is located where the cross stream gradient of $\overline{u'u'}$ is a maximum, that is to the inshore side of the maximum velocity shear. The zero crossing near the current axis is generally slightly on the cyclonic side of the current. A less well defined minimum of $\overline{u'v'}$ is found on the anticyclonic side of the current. These negative values approach zero and/or become positive at the southern edge of the current. The above statements do not hold at 138.0°E where apparent wide meandering of the current obscures the maximum and minimum.

The cross covariance (Figs. 4m, 5m, and 10), $\overline{u't'}$, changes significantly in this region and is positive through most of the region studied. A maximum found on the cyclonic side of the current may be a reflection of the maximum in the rms u'. The maximum oscillates in magnitude downstream until the current reaches Shionomisaki and then increases and becomes better defined east of Shionomisaki. The tem-

perature-velocity covariance, $\overline{v't'}$, is generally of much smaller magnitude than $\overline{u't'}$, due in part to the smaller rms fluctuation in the cross stream velocity (Figs. 4n and 5n).

The four horizontal kinetic energy transfer terms, $\overline{u'v'}\ \partial U/\partial y$, $\overline{u'u'}\ \partial U/\partial x$, $\overline{u'v'}\ \partial V/\partial x$, and $\overline{v'v'}\ \partial V/\partial y$, have been calculated. Examples of their cross section distribution can be seen in Figures 4 and 5. The first two terms, which involve the gradient of the downstream velocity component, U, are through most of the region locally of much larger magnitude than the second two terms which involve the cross stream velocity component, V.

A general cross stream variation of the term $\overline{u'u'}\ \partial U/\partial y$ is found throughout this region of the Kuroshio. As noted previously, $\overline{u'v'}$ changes sign from positive on the cyclonic side of the current, where $\partial U/\partial y$ is negative, to negative on the anticyclonic side of the current, where $\partial U/\partial y$ is positive. Due to this change in sign, $\overline{u'v'}\ \partial U/\partial y$ is negative across the current, i.e., this term tends to decrease the mean flow kinetic energy. A very narrow region, just on the cyclonic side of the current axis, of positive production, i.e., $\overline{u'v'}\ \partial U/\partial y$ is positive, is indicated on several sections. However, these values are not significantly different from zero. The magnitude of $\overline{u'v'}\ \partial U/\partial y$ is largest on the cyclonic side of the current where both $\overline{u'v'}$ and $\partial U/\partial y$ have their cross stream maximums in magnitude. This region of negative production increases in magnitude east of Shionomisaki.

The second leading kinetic energy transfer term is $\overline{u'u'}\ \partial U/\partial x$. Since $\overline{u'u'}$ is an order of magnitude larger than $\overline{u'v'}$ through the current, this term is often large even though $\partial U/\partial x$ is much smaller than $\partial U/\partial y$. Thus $\overline{u'u'}\ \partial U/\partial x$ is found to be a dominant term in much of the current although the error bounds are also correspondingly large—the average error in $\overline{u'u'}\ \partial U/\partial x$ is three times that for $\overline{u'v'}\ \partial U/\partial y$. Through this region of the Kuroshio, the term $\overline{u'u'}\ \partial U/\partial x$ has a positive maximum in the cyclonic side of the current. The maximum becomes better defined to the east of Shionomisaki. On the anticyclonic side $\overline{u'u'}\ \partial U/\partial x$ is generally negative. However, no well defined minimum is observed.

The terms $\overline{u'v'}\ \partial V/\partial x$ and $\overline{v'v'}\ \partial V/\partial y$ have been minimized to some extent by the choice of using local downstream coordinates. Few significant changes are readily apparent in either the cross or downstream directions for the term $\overline{u'v'}\ \partial V/\partial x$. The term $\overline{v'v'}\ \partial V/\partial y$ is generally negative in the same region on the cyclonic side of the current that $\overline{u'v'}\ \partial U/\partial y$ and $\overline{u'u'}\ \partial U/\partial x$ have their maximums.

In Figure 11 downstream averages of each of the transfer terms are plotted as a function of distance from the current axis. The plotted error is the average error reduced by a factor of $(n-1)^{-\frac{1}{2}}$ where n is the number of independent estimates. It is only on the cyclonic portion of the current that the two dominant terms are significantly nonzero. However, in this region they tend to cancel one another. The downstream average of $\overline{u'v'}\ \partial V/\partial x$ is everywhere not significantly greater than zero. The previously noted tendency for negative values of $\overline{v'v'}\ \partial V/\partial y$ on the cyclonic

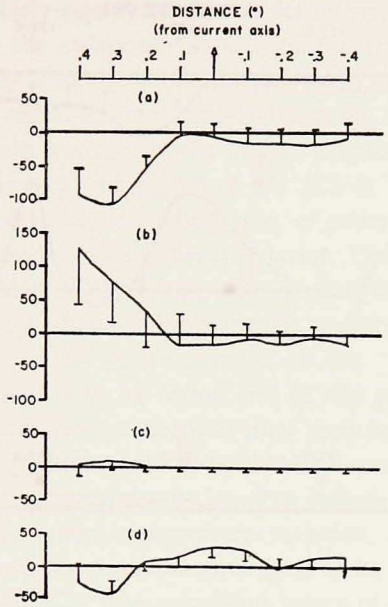

Figure 11. Downstream averages of the kinetic energy transfer components (10^{-4} cgs) versus distance (° latitude, positive is toward cyclonic side of current) from current axis. One of the symmetric error bounds is drawn. (a) $\overline{u'v'}\ \partial U/\partial y$, (b) $\overline{u'u'}\ \partial U/\partial x$, (c) $\overline{u'v'}\ \partial V/\partial x$, (d) $\overline{v'v'}\ \partial V/\partial y$.

side is now significant. However, the cross stream integral of this term is not significantly different from zero.

Cross stream averages of each of the kinetic energy transfer terms and the net kinetic energy transfer are presented as a function of longitude in Figure 12. The bounds used to define the edges of the current are 25 cm/s on the cyclonic side of the current and 60 cm/s on the anticyclonic side (as explained previously). The error estimates are the same as in Figure 11.

The strong dependence of the energy transfer on distance downstream is apparent. The term $\overline{u'v'}\ \partial U/\partial y$ is negative, i.e., energy flow from the mean flow to the fluctuations. The amplitude of this term is seen to increase east of Shionomisaki. The term $\overline{u'u'}\ \partial U/\partial x$ is primarily positive and has a wave-like appearance. No significant changes are observed downstream for the terms $\overline{u'v'}\ \partial V/\partial x$ or $\overline{v'v'}\ \partial V/\partial y$ due to their small amplitude compared to the error estimates. The total net energy transfer is dominated by the term $\overline{u'u'}\ \partial U/\partial x$. Regions of transfer of energy to the mean flow alternate downstream with regions of transfer to the fluctuations. The net kinetic energy transfer over the entire region, formed by a simple average of the cross stream averaged values of Figure 12, are presented in Table 3. These

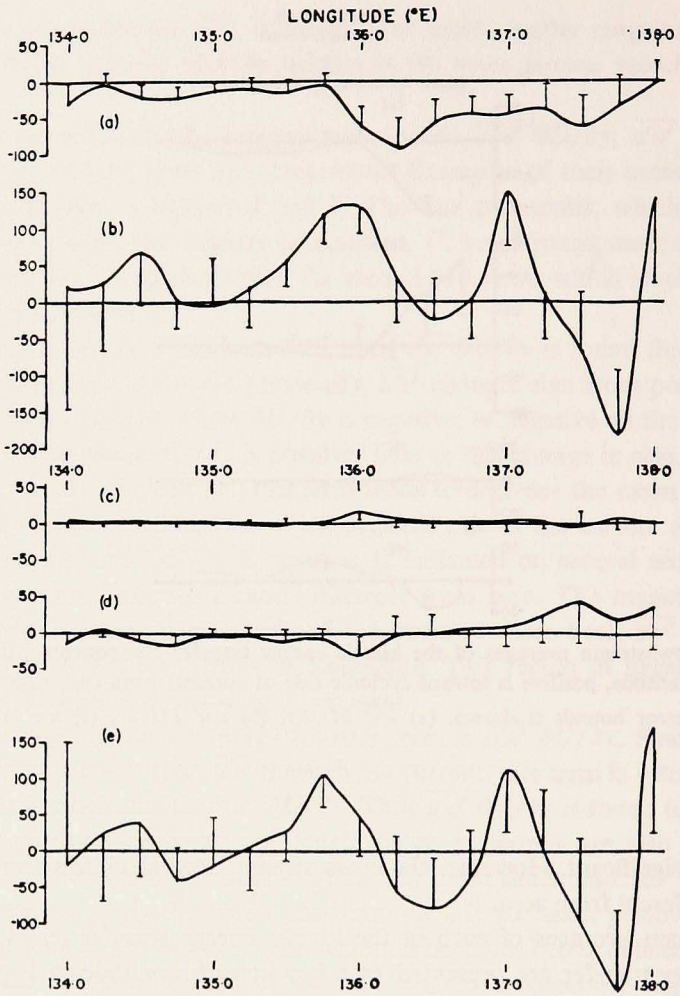

Figure 12. Cross stream averages of the kinetic energy transfer components (10^{-4} cgs) versus longitude (°E). One of the symmetric error bounds is drawn. (a) $\overline{u'v'}\ \partial U/\partial y$, (b) $\overline{u'u'}\ \partial U/\partial x$, (c) $\overline{u'v'}\ \partial V/\partial x$, (d) $\overline{v'v'}\ \partial V/\partial y$, (e) total kinetic energy transfer (sum of (a) - (d)).

Table 3. Net kinetic energy transfer (ergs cm^{-3} s^{-1}).

$\overline{u'v'}\ \partial U/\partial y$	$-.0034 \pm .0008$
$\overline{u'u'}\ \partial U/\partial x$	$.0029 \pm .0025$
$\overline{u'v'}\ \partial V/\partial x$	$.0002 \pm .0002$
$\overline{v'v'}\ \partial V/\partial y$	$.0002 \pm .0008$
Total Kinetic Transfer	$-.0001 \pm .0030$

numbers are not particularly significant due to the apparent wave-like character of the energy transfer and the overpowering size of the error. The result, however, demonstrates the difficulty involved in obtaining a 'good' estimate of the total kinetic energy transfer. The low signal-to-error ratio is due to the term $\overline{u'u'}\ \partial U/\partial x$. As mentioned previously this term has locally the largest magnitude and the largest error bounds. In averaging, the large magnitude of $\overline{u'u'}\ \partial U/\partial x$ is partially lost because it is both positive and negative but the large error, of course, remains. Compounding this problem is the near cancellation of the four terms. Thus, the sign of the resulting net energy transfer is lost within the error. Because of this cancellation, the terms $\overline{u'v'}\ \partial V/\partial x$ and $\overline{v'v'}\ \partial V/\partial y$, although having small magnitude locally, may be as important in the net transfer as $\overline{u'v'}\ \partial U/\partial y$ and $\overline{u'u'}\ \partial U/\partial x$.

The temperature variance transfer terms, $\overline{u't'}\ \partial T/\partial x$ and $\overline{v't'}\ \partial T/\partial y$, have been calculated by the same numerical methods as were used for the kinetic energy transfer. Thus, the mean temperature field is a 'climatic' mean, i.e., averaged over all seasons. The fluctuations in temperature therefore include the seasonal temperature variation. Since the total annual temperature variation, peak to peak, is roughly 10°C, if we consider the seasonal temperature cycle to be a sine wave, the temperature variance, $\overline{t't'}$, is 12.50(°C)^2. The calculated values of $\overline{t't'}$ range from 8-27(°C)^2, indicating that the dominant signal in the rms t' is due to seasonal influence. The covariances $\overline{u't'}$ and $\overline{v't'}$ will be biased by the seasonal temperature fluctuation if there is a correlation of the seasonal current speed and temperature fluctuations. There is a correlation between the seasonal velocity signal and the seasonal temperature signal (both being positive in summer and negative in winter). However, the seasonal velocity fluctuation peak to peak is approximately 50 cm/s (at the current axis) (Taft, 1972), and if we again use a sine wave to simply represent the seasonal velocity signal, $\overline{u'u'}$ due to the seasonal velocity fluctuation is only 312 cm^2/s^2. Then the seasonal rms u' is about 18 cm/s, which is much smaller than the rms u' in our results (which is about 45 cm/s at the current axis, $\overline{u'u'} \cong 2000$ cm^2/s^2). Thus, there is some hope that the covariance of the seasonal signals is less than the nonseasonal covariance.

Very little pattern in $\overline{u'u'}\ \partial T/\partial x$ or $\overline{v't'}\ \partial T/\partial y$ is found, due to the large error bounds, on the cross stream plots (Figs. 4 and 5). The downstream average of these two terms is plotted in Figure 13. Here we see some tendency for $\overline{u't'}\ \partial T/\partial x$ to be positive and $\overline{v't'}\ \partial T/\partial y$ to be negative on the cyclonic side of the current. The amplitude of the two terms is much less on the anticyclonic side of the current. The cross stream averaged results are plotted in Figure 14. Although the amplitudes are at all sections, except 137.00°E, less than the error, we can note that there is a tendency for both terms to cancel each other. The net values over the entire region are $\overline{u't'}\ \partial T/\partial x = (1.6 \pm 4)$ and $\overline{v't'}\ \partial T/\partial y = (-1.2 \pm 3)$ in units ((°C)^2/s) $\times\ 10^{-6}$. Thus, the same effect of cancellation noted for the kinetic energy transfer terms is found—the total transfer is an order of magnitude less than the leading terms.

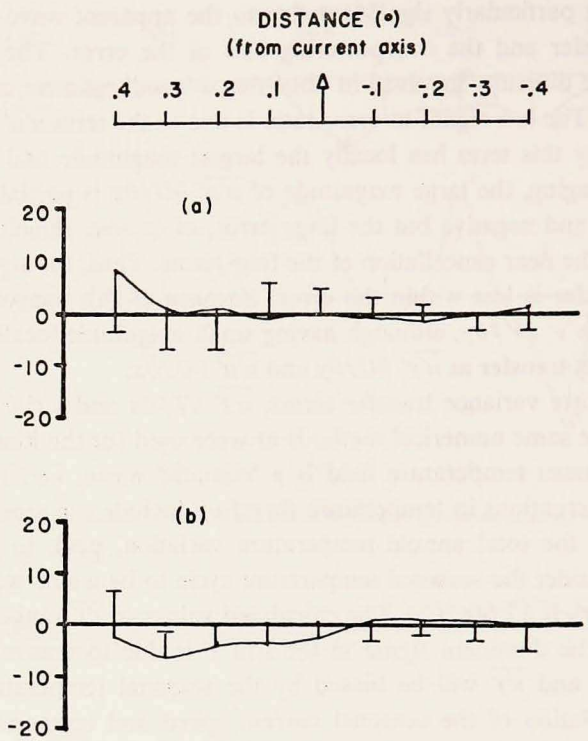

Figure 13. Downstream averages of the temperature variance transfer (10^{-6}(°C)^2/s) versus distance (° latitude, positive toward cyclonic side of current) from current axis. One of the symmetric error bounds is drawn. (a) $\overline{u't'}\,\partial T/\partial x$, (b) $\overline{v't'}\,\partial T/\partial y$.

The terms on the right-hand side of the fluctuating kinetic energy (FKE) equation (1), the kinetic energy transfer terms, also appear in the equation for the mean kinetic energy (MKE) but with opposite sign (compare for example Eq. 6.36 in Monin and Yaglom, 1971). Thus, if we call the transfer terms in the FKE equation source terms they appear as sink terms in the MKE equation. It is of interest then to inquire whether a downstream increase (decrease) in <FKE> is associated with a comparable decrease (increase) in <MKE>; here brackets denote cross stream average. In Figure 15 are illustrated the cross stream averages, <FKE> and <MKE>, as well as their sum, the total kinetic energy <TKE> as a function of longitude. It is important to note that the <TKE> is not constant along the current in this region. Between 135.0°E and 136.0°E, the <TKE> increases by about 50%. We believe, based on arguments presented in Teramoto (1971), that this large increase is qualitatively correct and is not solely an artifice of using a constant k-factor. It is not possible to determine if this increase of <TKE> is due to the potential energy transfer terms, because of the large uncertainties of the estimates (see Fig. 14). A possible source is the pressure work term (term (b) in Eq. (3)).

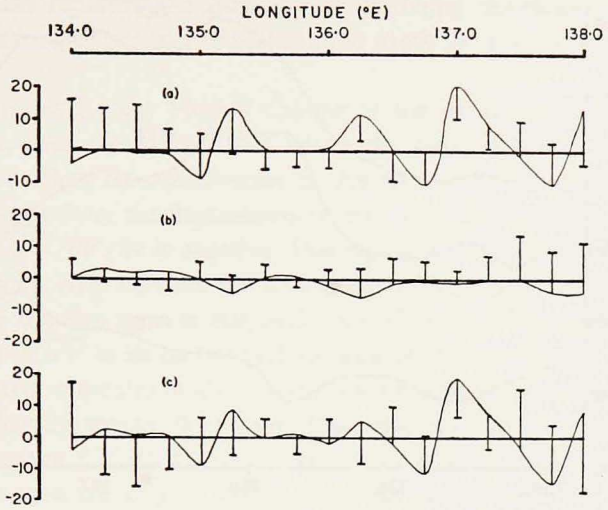

Figure 14. Cross stream averages of the temperature variance transfer (10^{-3}(°C)^2/s) versus longitude (°E). One of the symmetric error bounds is drawn. (a) $\overline{u't'}\ \partial T/\partial x$, (b) $\overline{v't'}\ \partial T/\partial y$, (c) total transfer (sum of (a) + (b)).

However, with our data set we are unable to estimate this term. Nonetheless, from Figure 15 we note that a downstream increase (decrease) in <FKE> coincides with a downstream decrease (increase) in <MKE>.

In the following we estimate whether some of the downstream variations in <FKE> and <MKE> in Figure 15 are consistent with our previous estimates of the transfer terms. The substantial derivatives of <FKE> and <MKE> are estimated by $<U\ \partial/\partial x\ (\ )>$ which in turn are approximated by $<U>\ \partial/\partial x\ <(\ )>$. For $<U>$ we take 100 cm/s. The energy gradients in the region from 136.25°E to 138.0°E have been estimated by straight lines (fit by eye) to the graphs of Figure 15. Using the above approximations we estimate that in this region 90×10^{-4} ergs/cm^{3}s of <MKE> are being lost by the current while the <FKE> is increasing at a rate of 52×10 ergs/cm^{3}s. In this region the calculated transfer of kinetic energy due to the term $\overline{u'u'}\ \partial U/\partial x$ has large downstream oscillations (see Fig. 12) and the GEK depth-bias may add large errors to this transfer term. Therefore we ignore this term in the following comparison and examine the other dominant term $\overline{u'v'}\ \partial V/\partial y$. The average of $\overline{u'v'}\ \partial U/\partial y$ in this region is -50×10^{-4} ergs/cm^{3}s. Thus, this term accounts for approximately 100% of the increase in <FKE> and 55% of the decrease in <MKE>. Similar estimates in the region 135.25°E to 135.75°E where there are large downstream gradients of energy have been made. Here the <MKE> is increasing at a rate of 273×10^{-4} ergs/cm^{3}s, the <FKE> is decreasing at a rate of 44×10^{-4} ergs/cm^{3}s. In this region the GEK bias in the term $\overline{u'u'}\ \partial U/\partial x$ is not

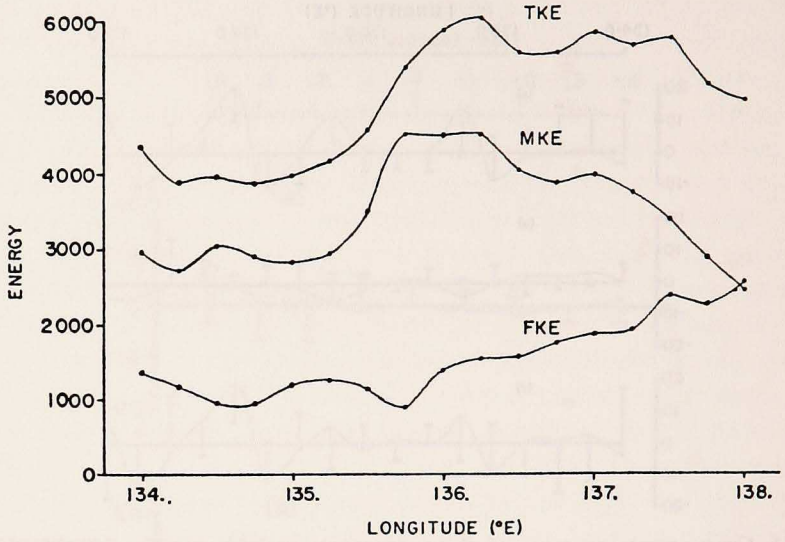

Figure 15. Cross stream averages of the mean kinetic energy (MKE), the fluctuation kinetic energy (FKE), and the total kinetic energy (TKE = MKE + FKE). Units ergs/cm^{3}s.

significant, so we may compare the total kinetic energy transfer, 50×10^{-4} ergs/cm^{3}s, to the downstream changes in energy. Thus, the kinetic energy transfer terms account for about 25% of the increase in <MKE> and 100% of the decrease in <FKE>.

4. Conclusions

In this paper we have been able to calculate in more detail the terms in the fluctuating kinetic energy equation for the surface layer of the Kuroshio south of Japan than has been possible for the Florida Current. In general our results support the findings for the Florida Current.

We have calculated the four horizontal kinetic energy transfer terms and found $\overline{u'v'}\,\partial U/\partial y$ and $\overline{u'u'}\,\partial U/\partial x$ to be of the largest magnitude and usually with the opposite sign. The comparable and dominant terms for the Florida Current are $\overline{u'v'}\,\partial V/\partial x$ and $\overline{v'v'}\,\partial V/\partial y$. Significant downstream changes in the cross stream averages of the dominant terms have been found. As for the Florida Current (Hager, 1977) we have found that estimates of the downstream variability in the total conversion rate of mechanical energy are dominated by the downstream transfer term $\overline{u'u'}\,\partial U/\partial x$ ($\overline{v'v'}\,\partial V/\partial y$ for the Florida Current). This last result, not anticipated when this study was begun, is somewhat unfortunate since the error of estimate of the downstream transfer term, which is much larger than that of $\overline{u'v'}\,\partial U/\partial y$, is too large in certain regions to permit a significant areal average to be formed. Brooks and

Niiler (1977) also reported the difficulty in obtaining significant results for the energy transfer averaged across and through the depth for one section of the Florida Current.

A persistent result for the Florida Current is the existence of a region on the cyclonic portion, near the current axis where the cross stream transfer term $\overline{u'v'}\ \partial V/\partial x$ is positive. Here the contribution of this term to the kinetic energy balance is to transfer energy from the fluctuations to the mean flow and the so-called eddy viscosity $K_H = -\overline{u'v'}/\partial V/\partial x$ is negative. This region can be identified in a plan view of the current as the strip between the zero contour line of $\overline{u'v'}$ and the stream axis. The comparable transfer term in our study is $\overline{u'v'}\ \partial U/\partial y$. We note a tendency of the zero contour of $\overline{u'v'}$ to lie on the cyclonic side of the current axis (Fig. 9). However, when the error estimates in $\overline{u'v'}$ and $\partial U/\partial y$ are included, the cross stream transfer is not significantly greater than zero. This result also holds in the non-rotated coordinates except at 135.75°E, where significant positive transfer was found. A tendency for the zero crossing of $\overline{u'v'}$ to occur on the cyclonic side of the current axis has also been noted in laboratory studies of asymmetric turbulent wall jets (Hanjalic and Launder, 1972).

We have also estimated the downstream changes in the cross stream averaged mean kinetic energy <MKE> and fluctuation kinetic energy <FKE>. In two regions of the current, changes in <MKE> and <FKE> have been related to the transfer terms. From these results we can conclude that the energy transfer terms are important in the energy balance equations and account for 25-55% of the calculated rates of increase or decrease of <MKE> (100% for <FKE>) in these regions of the Kuroshio.

Several of our calculations have been severely limited by the quantity and accuracy of the data. The constant k-factor used in converting the GEK measurements severely limits confidence in the $\overline{u'u'}\ \partial U/\partial x$ results for the portions of the region where the depth changes rapidly downstream (136.0°E to 137.0°E). The temperature variance transfer terms $\overline{u't'}\ \partial T/\partial x$ and $\overline{v't'}\ \partial T/\partial y$ have been calculated but interpretation of the results is difficult due to dominance of the seasonal signal and low signal-to-noise ratio. We note that there is a significant downstream fluctuating heat flux, i.e., $\overline{u't'} > 0$, through most of the current as found for the Florida Current (Brooks and Niiler, 1975, 1977). However, our results may be due to the seasonal, positive correlation of u' and t'. When more data are available and significant calculations can be made for seasons, the role of the terms will be better defined.

Acknowledgments. We especially thank T. F. Webster, who initiated this research, for his encouragement and support during the long course of this research. P. P. Niiler and W. Sturges III are sincerely thanked for their helpful suggestions and discussion. This research was supported by the Office of Naval Research under Contract No. N00014-75-C-0201. Lastly, and most importantly, we thank our wives for their assistance and encouragement.

REFERENCES

Brooks, I. H. and P. P. Niiler. 1975. The Florida Current at Key West: summer 1972. J. Mar. Res., *33,* 83–92.

—— 1977. Energetics of the Florida Current. J. Mar. Res., *35,* 163–191.

Hager, J. G. 1977. Kinetic energy exchange in the Gulf Stream. J. Geophys. Res., *82,* 1718–1724.

Hanjalic, K. and B. E. Launder. 1972. Fully developed asymmetric flow in a plain channel. J. Fluid Mech., *51,* 301–336.

Monin, A. S. and A. M. Yaglom. 1971. Statistical Fluid Mechanics: Mechanics of Turbulence, Vol. 1. The MIT Press, Cambridge, 769 pp.

Niiler, P. P. and A. R. Robinson. 1967. The theory of free inertial jets. II. A numerical experiment for the path of the Gulf Stream. Tellus, *19,* 601–619.

Oort, A. H. 1964. Computation of the eddy heat and density transports across the Gulf Stream. Tellus, *19,* 55–63.

Orlanski, I. 1969. The influence of bottom topography on the stability of jets in a baroclinic fluid. J. Atmos. Sci., *26,* 1216–1232.

Robinson, A. R. and P. P. Niiler. 1967. The theory of free inertial current. I. Path and structure. Tellus, *19,* 269–291.

Robinson, A. R. and B. A. Taft. 1972. A numerical experiment for the path of the Kuroshio. J. Mar. Res., *30,* 65–101.

Schmitz, W. J. and P. P. Niiler. 1969. A note on the kinetic energy exchange between fluctuations and the mean flow in the surface layer of the Florida Current. Tellus, *21,* 814–819.

Szabo, D. 1978. Energetics of the Kuroshio south of Japan. Department of Oceanography, Florida State University. M.S. Thesis. 78 pp.

Taft, B. A. 1972. Characteristics of the flow of the Kuroshio south of Japan, *in*: Kuroshio: Physical Aspects of the Japan Current, H. Stommel and K. Yoshida, eds. University of Washington Press, Seattle, 517 pp.

Teramoto, T. 1971. Estimation of sea-bed conductivity and its influence upon velocity measurements with towed electrodes. J. Oceanogr. Soc. Japan, *27,* 7–19.

Webster, F. 1961. The effects of meanders on the kinetic energy balance of the Gulf Stream. Tellus, *13,* 392–401.

—— 1965. Measurements of eddy fluxes of momentum in the surface layer of the Gulf Stream. Tellus, *17,* 239–245.

White, W. B. and J. P. McCreary. 1976. On the formation of the Kuroshio meander and its relationship to the large-scale ocean circulation. Deep-Sea Res., *23,* 33–47.

Worthington, L. V. and J. Kawai. 1972. Comparison between deep sections across the Kuroshio and the Florida Current and Gulf Stream, *in*: Kuroshio: Physical Aspects of the Japan Current. H. Stommel and K. Yoshida, eds. University of Washington Press, Seattle, 517 pp.

Received: *28 July, 1978;* revised: *1 May, 1979.*